Substrate-Induced Conformational Change of the Escherichia coli Membrane Insertase YidC

ARTICLE *in* BIOCHEMISTRY · JULY 2009

Impact Factor: 3.02 · DOI: 10.1021/bi9003809 · Source: PubMed

6 AUTHORS, INCLUDING:

Tilmann Roos
Hohenheim University
6 PUBLICATIONS **197** CITATIONS
SEE PROFILE

Andreas Kuhn
Hohenheim University
109 PUBLICATIONS **3,776** CITATIONS
SEE PROFILE

Uwe Gerken
University of Bayreuth
24 PUBLICATIONS **312** CITATIONS
SEE PROFILE

6684 *Biochemistry* **2009,** *48,* 6684–6691
DOI: 10.1021/bi9003809

BIOCHEMISTRY
including biophysical chemistry & molecular biology
Article

Substrate-Induced Conformational Change of the *Escherichia coli* Membrane Insertase YidC[†]

Sophie Winterfeld, Nora Imhof, Tilmann Roos, Gerda Bär, Andreas Kuhn, and Uwe Gerken*

Institute of Microbiology, University of Hohenheim, Garbenstrasse 30, D-70599 Stuttgart, Germany

Received March 6, 2009; Revised Manuscript Received June 8, 2009

ABSTRACT: The membrane insertase YidC from *Escherichia coli* reversibly binds its substrate Pf3 coat protein. The effect of this initial binding process was examined in vitro by fluorescence quenching of the tryptophan (Trp) residues of YidC which are highly sensitive fluorescent probes for changes of the protein's tertiary structure. Membrane-reconstituted (in DOPC or DOPE/DOPG vesicles) as well as detergent-solubilized (C_{12}PC) YidC was titrated with a Trp-free Pf3 coat mutant. Quenching of the intrinsic Trp fluorescence after titration indicates a change in the tertiary structure of YidC upon binding to the Pf3 coat substrate. Analysis of the binding curves taken from the fluorescence data yielded values for the dissociation constant (K_D) in the range of 0.5−1.8 μM. Titration experiments with two Trp mutants reveal that the change in the tertiary structure involves mainly the membrane-spanning domain. The influence of the different environments on the secondary structure of YidC as well as of the YidC large periplasmic domain (P1) was investigated by circular dichroism (CD). The CD data show that the YidC secondary structure changes upon reconstitution into a membrane environment when compared to the detergent-solubilized state. In particular, the P1 domain of YidC is considerably affected by the detergent C_{12}PC. This underlines the importance to study conformational changes with membrane-inserted proteins.

During the membrane insertion process of the newly synthesized coat protein of the filamentous phage Pf3, the protein first binds to YidC and then adopts a transmembrane conformation in the membrane bilayer. YidC is a six-spanning membrane protein of *Escherichia coli* and has homologues in mitochondria and chloroplasts (*1*). The proposed membrane topology of YidC is displayed in Figure 1 (*2*) and shows a large periplasmic domain that is located between TM1 and TM2. In mitochondria, Oxa1 is the only enzyme that inserts proteins from the matrix into the inner membrane since mitochondria lack the Sec translocase. In bacteria, most proteins are inserted by the Sec translocase with the help of YidC (*3*). However, a few Sec-independent proteins use the YidC-only pathway for membrane insertion. Among these are the filamenteous phage coat proteins (*4*), subunit c of the ATP synthase (*5*), the mechanosensitive channel protein MscL (*6*), and components of respiratory complexes (*7*).

The Pf3 coat protein is the smallest of the YidC substrates and consists of 44 amino acid residues. The transmembrane region of 18 hydrophobic residues is flanked by an N-terminal negatively charged periplasmic region of 18 residues and a positively charged cytoplasmic region of eight residues at the C-terminus. The negatively charged residues are important for the translocation of the N-terminal domain into the periplasm (*8*). Binding of the Pf3 coat protein to YidC on its cytoplasmic face allows the protein to insert into the membrane bilayer before it is assembled with the phage DNA into the viral particles. The binding of the Pf3 coat protein to YidC involves most likely transmembrane regions TM1 and TM3 of YidC since cysteine residues at specific positions in YidC were cross-linked to a Pf3 coat derivative that has a single cysteine in its transmembrane region (*9*). The cross-links are located in the center of the transmembrane regions, suggesting that binding to YidC is mainly driven by hydrophobicity.

We have previously shown that the Pf3 coat protein binds reversibly to detergent-solubilized YidC and verified that the binding process is dominated by hydrophobic interactions (*10*). In this study, we analyzed in detail the binding reaction of the Pf3 coat protein to membrane-reconstituted YidC. Proteoliposomes containing purified YidC were titrated with a tryptophan-free mutant Pf3 coat protein, and the binding was monitored by quenching of the intrinsic Trp fluorescence of the YidC protein. In addition, the membrane reconstitution of YidC was spectroscopically analyzed by measuring the intrinsic Trp fluorescence and circular dichroism (CD).[1] We show that the binding of the

[†]Financial support was provided by DFG Grant Ku 749.

*To whom the correspondence should be addressed. Telephone: ++49-711-459 23885. Fax: ++49-711-459 22238. E-mail: gerken@uni-hohenheim.de.

[1]Abbreviations: ANS, 1-anilinonaphthalene-8-sulfonate; CD, circular dichroism; cmc, critical micelle concentration; DDM, dodecyl maltoside; DOPC, 1,2-dioleoyl-*sn*-glycero-3-phosphocholine; DOPE, 1,2-dioleoyl-*sn*-glycero-3-phosphoethanolamine; DOPG, 1,2-dioleoyl-*sn*-glycero-3-[phospho-*rac*-(1-glycerol)]; C_{12}PC, *n*-dodecylphosphocholine; ECL, enhanced chemiluminescence; EDTA, ethylenediaminetetraacetic acid; IPTG, isopropyl β-thiogalactopyranoside; LB, Luria broth; PBS, phosphate-buffered saline; PM, photomultiplier; PMSF, phenylmethanesulfonyl fluoride; PPB, potassium phosphate buffer; SDS, sodium dodecyl sulfate; SEC, size exclusion chromatography; TBS, Tris-buffered saline; Tris, 2-amino-2-(hydroxymethyl)-1,3-propanediol.

 Published on Web 06/09/2009

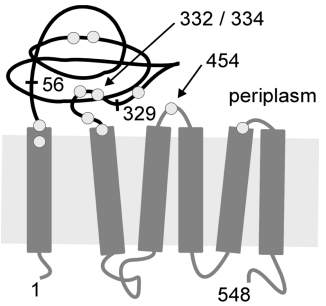

FIGURE 1: Membrane topology of YidC with its large periplasmic domain P1 (colored black). The numbers in this domain indicate the positions of the amino acid residues flanking the segment of P1 which was used in this work. The approximate positions of the 11 Trp residues along the structure are marked by circles, and the residues left in the Trp mutants $YidC_{W332/W334}$ and $YidC_{W454}$ are denoted with arrows.

Pf3 coat protein to the reconstituted YidC induces a conformational change. The binding of the Pf3 coat protein is reversible with a dissociation constant K_D in the same range as that of solubilized YidC in detergent. We also show that the choice of the detergent which is used for solubilization of YidC is crucial for maintaining the correct folding of periplasmic domain P1.

MATERIALS AND METHODS

Expression and Purification of Wild-Type YidC. Wild-type *E. coli* YidC (with a C-terminal His_{10} tag) was cloned into pMS119EH (*11*) and transformed into *E. coli* C41 cells, and the cells were grown aerobically in flasks in LB medium at 37 °C to an optical density (OD_{600}) of 0.6. Protein expression was induced with 0.5 mM IPTG for 3 h at 37 °C. The cells were harvested at 5000*g* and 4 °C, resuspended in 1 mL of 2-amino-2-(hydroxymethyl)-1,3-propanediol (Tris)-HCl buffer [20 mM Tris-HCl (pH 8.0), 1 mM EDTA, and 20% sucrose] per gram cells, and broken with a French pressure cell at 8000 psi after the addition of protease inhibitor PMSF at 1 mM. Cell debris was separated from the crude lysate at 6000*g* and 4 °C, and the membrane fraction was collected by centrifugation for 40 min at 150000*g* and 4 °C. The membranes were homogenized in PBS at pH 7.4 and stored at −80 °C. YidC was purified following the protocol of Molina et al. (*12*) with minor changes. The membranes were solubilized on ice for 3 h with 1% (w/v) dodecyl maltoside (DDM) (GERBU Biochemicals GmbH) in 150 mL of potassium phosphate buffer (PPB) [20 mM PPB (pH 7.4), 300 mM NaCl, and 40 mM imidazole] and centrifuged at 150000*g* and 4 °C for 30 min to remove all nonsolubilized components. YidC was purified on a Ni^{2+}-affinity column (Qiagen) followed by size exclusion chromatography (SEC) using a Superdex 200 16/60 column (GE Healthcare) in sodium acetate buffer [100 mM NaCl (pH 5.2)]. The peak containing monomeric YidC was concentrated by ultrafiltration at 4 °C using an Amicon Ultra device (Millipore) with a 30 kDa cutoff. Purified YidC was analyzed for homogeneity and homodispersity by SEC using a Superdex 200 10/300 column (GE Healthcare).

The His_{10}-tagged wild-type *E. coli* YidC was also purified in *n*-dodecylphosphocholine ($C_{12}PC$) (Anatrace, Inc.) as described previously (*10*).

Generation, Expression, and Purification of YidC Trp Mutants. Mutants $YidC_{W332/W334}$ and $YidC_{W454}$ (both with a C-terminal His_{10} tag) were obtained after site-directed mutagenesis (*8*) to change all Trp residues into Phe with the exception of the indicated residues. The mutants were cloned into pMS119EH (*11*), transformed into *E. coli* C43 cells, and purified in DDM as described previously (*10*). Both mutants are functional since they complemented the $YidC^-$ phenotype of *E. coli* MK6.

Expression and Purification of YidC Domain P1. Water-soluble YidC periplasmic domain P1 was expressed and purified as described by Ravaud (*13*). Ni^{2+}-affinity purified protein was analyzed for homogeneity and homodispersity by SEC using a Superdex 200 10/300 column (GE Healthcare). The monomeric fractions were pooled and concentrated by ultrafiltration at 4 °C using an Amicon Ultra device (Millipore).

For the intrinsic Trp fluorescence and CD measurements of detergent-solubilized YidC and the P1 domain, it was necessary to remove all traces of imidazole remaining after the Ni^{2+}-affinity step from the YidC samples. For this purpose, ≈350 μL of the sample was dialyzed overnight against 100 mL of the respective buffer required for the actual experiment. For the experiments with detergent-solubilized YidC, the buffers contained 1.2 mM $C_{12}PC$ or 0.36 mM DDM.

The purities of all purified proteins were confirmed using sodium dodecyl sulfate−polyacrylamide gel electrophoresis (SDS−PAGE) followed by staining with Coomassie Blue R250, and the concentrations were determined using the method of Lowry and Peterson (*14*).

Expression and Purification of Pf3 Coat Protein Mutants. The tryptophan-free mutant Pf3W0 coat protein as well as the mutant $Pf3_{19A}$ coat protein, in which the membrane-spanning region (residues 19−34) was replaced with 19 alanine residues, were expressed from *E. coli* C41 cells bearing plasmid pMS119HE with the *pf3coat* gene as described previously (*15*).

Preparation of Phospholipids. 1,2-Dioleoyl-*sn*-glycero-3-phosphocholine (DOPC), 1,2-dioleoyl-*sn*-glycero-3-phosphoethanolamine (DOPE), and 1,2-dioleoyl-*sn*-glycero-3-[phospho-*rac*-(1-glycerol)] (DOPG) were purchased from Avanti Polar Lipids (Alabaster, AL). A total amount of 60 mg of DOPC and 60 mg of a DOPE/DOPG mixture (3:1, w/w) were each dissolved in 2 mL of CH_2Cl_2 and dried for 6 h as a thin film under vacuum as described previously (*16*). The lipid films were resuspended in 4 mL of H_2O, frozen with liquid nitrogen, and then stored at −80 °C. Phosphate determination of the DOPC and DOPE/DOPG samples was performed according to Ames and Dubin (*17*). To generate the vesicles, 3.2 mM DOPC and DOPE/DOPG suspensions were treated by sonication with a microtip (Branson) on ice for several minutes until translucency was reached.

Membrane Reconstitution of YidC. YidC was reconstituted into membrane vesicles following the method described by Rigaud et al. (*18*) using the DOPC and DOPE/DOPG (3:1, w/w) phospholipid vesicles mixed with DDM at a molar ratio of 1:1. For reconstitution, 500 μM phospholipids pre-equilibrated with DDM were mixed with 2 μM YidC in DDM. The solution was allowed to equilibrate for 2.5 h at 4 °C under gentle mixing. The detergent was removed in 2 h via addition of 30 mg of Bio-Beads SM-2 (Bio-Rad Laboratories) at 4 °C. The proteoliposomes were separated by centrifugation for 10 min at 120000*g*, and the pellet was resuspended in Tris-HCl buffer [20 mM Tris-HCl (pH 7.0) and 100 mM NaCl] or 10 mM PPB (pH 7.0). With this protocol, a molar lipid to protein ratio of ∼300:1 was achieved.

Topology Analysis. Proteoliposomes (prepared as described above) were resuspended in 100 μL of Tris-HCl buffer [20 mM Tris-HCl (pH 7.0) and 200 mM NaCl]. Trypsin was added to a

final concentration of 2.5 μM, and proteolysis was conducted on ice for 1.5 h and terminated by precipitation with 15% (v/v) trichloroacetic acid (TCA). The sample was centrifuged and washed twice with acetone and subsequently analyzed by SDS−PAGE. For a control, an aliquot was digested in the presence of 10% (w/v) SDS.

The SDS gel was blotted onto a nitrocellulose membrane (Perkin-Elmer), and the membrane was blocked in Tris-buffered saline (TBS, pH 7.4) containing 5% (w/v) nonfat milk for 1 h at room temperature. After being washed, the membrane was consecutively incubated with the primary and secondary antibody, both diluted in TBS (pH 7.4) containing 0.05% Tween 20 and 4% (w/v) nonfat milk, for 1−1.5 h at room temperature. As the primary antibody, we used a polyclonal rabbit antibody recognizing periplasmic domain P1. The ECL (Millipore Corp.)-exposed film was quantified using Kodak Image Station 440 software.

Measurement of the Circular Dichroism (CD). The CD measurements were performed with a spectropolarimeter (Jasco 715) using quartz cuvettes (Hellma AG) with path lengths of 1 and 0.5 mm for the reconstituted and solubilized proteins, respectively. The sample holder was modified such that the cuvettes could be placed directly in front of the entrance window of the photomultiplier (PM). This arrangement avoids effects caused by differential scattering of turbid samples (*19*). All CD spectra were recorded in the range of 185−260 nm with a step width of 1 nm and a scanning speed of 20 nm/min. The signal-to-noise ratio was improved by choosing a response time of 4 s and an excitation bandwidth of 2 nm. Additionally, each spectrum was recorded at least three times.

All experiments were performed in 10 mM PPB buffer at pH 7.0 and 6.0 for the YidC samples and the P1 domain, respectively. The samples were diluted until the dynode voltage indication of the PM tube, which is a measure of the sample's linear absorbance, did not exceed 650 V during the complete scan. The spectra of detergent-solubilized and water-soluble proteins were background-corrected by subtracting a buffer blank spectrum, whereas the spectra of the reconstituted proteins were corrected with a spectrum of a sample containing DOPC or DOPE/DOPG vesicles only. The collected spectra were smoothed with the Savitzky−Golay filter, and first-derivative analysis was used to determine the minima and maxima of the spectra. To compare results from different samples, all spectra were normalized to the mean residue weight ellipticity (θ_{MRW}) [deg cm^2 /dmole] with

$$\theta(\lambda)_{MRW} = \frac{\theta(\lambda)_{mdeg}}{10cnd}$$

where $\theta(\lambda)_{mdeg}$ is the recorded spectra in millidegrees, d is the path length of the cuvette in centimeters, n is the number of amino acid residues, and c is the sample concentration in moles per liter. The concentration of each sample was determined after the experiment (*14*), and its purity was confirmed using SDS−PAGE followed by staining with Coomassie Blue R250.

Measurement of Fluorescence Spectra, Fluorometric Titration, and Data Analysis. The fluorescence measurements and titration experiments were performed at a constant temperature of 25 °C in the same setup as previously described (*10*). The tryptophan (Trp) residues of YidC were excited at 295 nm, and fluorescence spectra were recorded in the range of 305−420 nm with a step width of 1 nm and an integration time of 1 s. The slit widths of the excitation and detection monochromator were set to a spectral width of 2 and 3 nm, respectively. Fluorescence spectra were analyzed by fitting the background-corrected spectra $F(\lambda)$ to the log-normal distribution (*20*)

$$F(\lambda)_{log-normal} = F_0 \exp\left(\frac{\ln 2}{\ln^2 \rho} \ln^2\left[1 + \frac{(\lambda - \lambda_{max})(\rho^2 - 1)}{\rho\Gamma}\right]\right) \quad (1)$$

where F_0 is the fluorescence maximum value at λ_{max}, Γ is the line width (full width at the half maximum intensity), and ρ is the line shape asymmetry parameter.

C_{12}PC-solubilized and reconstituted YidC was titrated by stepwise addition of small aliquots (2−5 μL) of a 26 μM Pf3W0 coat stock solution. YidC was at a concentration of ~0.1 μM in 20 mM Tris-HCl buffer containing 10% (v/v) 2-propanol [Tris-HCl (pH 8.0) and 50 mM NaCl for the solubilized YidC and Tris-HCl (pH 7.0) and 100−250 mM NaCl for the reconstituted samples]. After each addition of Pf3W0 coat protein, the solution was allowed to equilibrate for 5 min, and subsequently, a fluorescence spectrum was recorded. All spectra were background-corrected by subtraction of a buffer blank spectrum. The binding curves were constructed by taking the fluorescence values F at the maxima and plotting $\Delta F_i = |F_i(1 + V_i/V_0) - F_0|$ against the molar substrate concentration, where F_i is the fluorescence value at the ith titration step and F_0 is the initial fluorescence value of YidC without substrate. Because of the increasing sample volume during the titration, the fluorescence values had to be corrected by the factor $1 + V_i/V_0$, where V_i is the total added volume at the ith titration step and V_0 is the initial volume. The dissociation constant K_D was obtained by fitting the binding curve to the hyperbolic equation

$$\Delta F = \Delta F_{max} \frac{[Pf3]}{[Pf3] + K_D} \quad (2)$$

where ΔF_{max} is the maximum fluorescence change at saturation. All linear and nonlinear least-squares fitting procedures were performed with the commercial software packages Origin 6.1 (OriginLab Corp.) and SigmaPlot 2000 (SPSS Inc.).

Since the $Pf3_{19A}$ coat protein still contains a Trp residue at the original position, the recorded spectra were corrected for the additional fluorescence. To do this, a parallel experiment in which a buffer blank in an identical cuvette was titrated by identical aliquots of $Pf3_{19A}$ coat protein was performed. The respective fluorescence spectrum was subtracted from the spectrum of the YidC-containing sample recorded for each corresponding titration step. The corrected spectra were further analyzed as described above.

In the titration experiment with C_{12}PC-solubilized YidC, the detergent concentration was kept below the critical micellar concentration (cmc) of C_{12}PC (1.2 mM) to prevent interactions between the Pf3 protein and the detergent molecules (*10*).

RESULTS

Conformational States of Soluble and Membrane-Reconstituted YidC. The six-spanning membrane protein YidC contains 11 tryptophan residues, all located on the periplasmic side (Figure 1). Fluorescence and CD spectroscopy were used to characterize the solubilized (YidC in C_{12}PC and YidC in DDM) and reconstituted (YidC in DOPC and YidC in DOPE/DOPG vesicles) states of YidC.

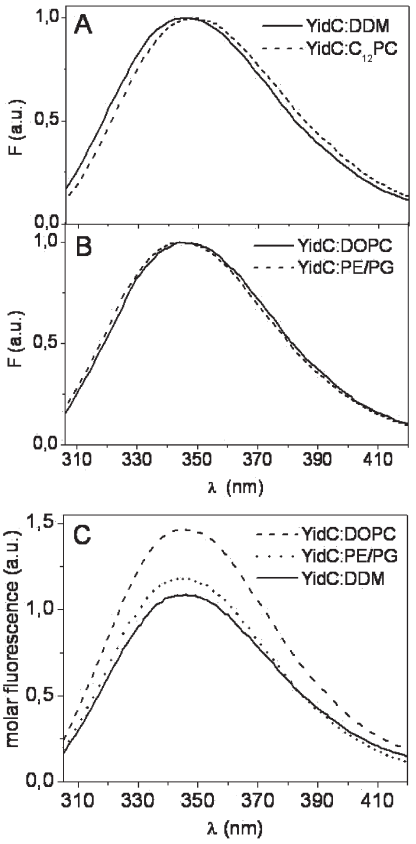

FIGURE 2: Normalized intrinsic Trp fluorescence spectra of (A) detergent-solubilized (DDM and $C_{12}PC$) and (B) membrane-reconstituted [DOPC and DOPE/DOPG (3:1, w/w)] YidC. (C) Intrinsic fluorescence per mole of DDM-solubilized and reconstituted YidC [DOPC and DOPE/DOPG (3:1, w/w)] [in 10 mM PPB (pH 7.0)].

Typical spectra of the intrinsic trytophan fluorescence of the detergent-solubilized and reconstituted YidC are shown in Figure 2A,B. The line shapes could be fitted with good accuracy to eq 1 (data not shown). The spectral position of the fluorescence peak is dependent on the protein environment. YidC in $C_{12}PC$ exhibits a fluorescence spectrum with a peak at a λ_{max} of 348 nm and a width Γ of 64.5 nm, whereas the spectrum of YidC in DDM is blue-shifted by ≈3 nm to a λ_{max} of 345 nm and has a width similar to that for YidC in $C_{12}PC$. The fluorescence spectra of membrane-reconstituted YidC show for both membrane environments fluorescence peaks at a λ_{max} of 345 nm and line widths of 61.7 and 62.7 nm for DOPC and DOPE/DOPG vesicles, respectively.

For the reconstituted YidC samples, the observed blue shift is accompanied by an increase in the intrinsic fluorescence per mole compared to that of the DDM-solubilized state (Figure 2C). A blue shift and an increase in the quantum yield are indicative of a change of the Trp residues to a more hydrophobic environment and hence strong spectroscopic indications of successfully reconstituted protein.

To examine the influence of the different environments on the secondary structure of YidC, the CD of YidC and the CD of periplasmic loop P1 of YidC (residues 56−329) were measured in the region between 185 and 260 nm. Panels A and B of Figure 3 show CD spectra of detergent-solubilized and membrane-reconstituted YidC, respectively. For the solubilized proteins (Figure 3A), both spectra exhibit rather similar shapes and amplitudes. Both spectra had minima at 220 and 209 nm, with the latter being significantly pronounced for YidC in $C_{12}PC$.

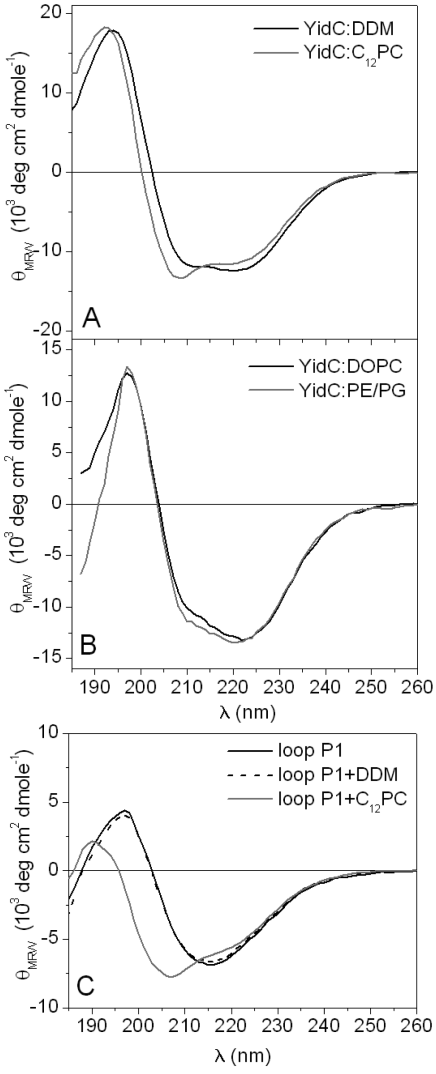

FIGURE 3: Circular dichroism spectra of (A) detergent-solubilized (DDM and $C_{12}PC$) and (B) membrane-reconstituted YidC [DOPC and DOPE/DOPG (3:1, w/w)] [in 10 mM PPB (pH 7.0)]. (C) Circular dichroism spectra of the P1 domain in the absence of detergent and in the presence of 0.48 mM DDM and 4.5 mM $C_{12}PC$ [in 10 mM PPB (pH 6.0)].

Furthermore, the maximum in the spectrum of YidC in $C_{12}PC$ is blue-shifted by ≈2 nm in comparison to that of YidC in DDM. In contrast, the spectra of the membrane-reconstituted samples (Figure 3B) show that the first minimum at 209 nm disappeared, and a red shift of the whole spectrum occurred by ≈3 nm when compared to the spectra in Figure 3A. In comparison to the spectra in Figure 3A, the observed disappearance of the minimum and the decrease in the amplitude of the positive band suggest that a significant fraction of α-helical structure is induced by the interaction with the detergent and disappears upon membrane reconstitution. This was confirmed by measuring CD spectra of periplasmic loop P1 in the presence of 4.5 mM $C_{12}PC$ and 0.48 mM DDM. These concentrations correspond to approximately 3 times the cmc of both detergents. The spectrum of free P1 is shown in Figure 3C (black spectrum). With its single broad negative band centered at 216 nm, the spectrum is typical for a protein with a predominant β-structure that has previously been proven by X-ray crystallography (*13*, *21*). In the presence of DDM, the secondary structure of the protein remained unchanged (dashed spectrum), whereas the presence of $C_{12}PC$

leads to the appearance of a second negative band at 206 nm (gray spectrum). Thus, C_{12}PC interacts with the loop, leading to a considerable change in its secondary structure. Because of the spectral position and intensity of this band, we conclude that the minimum at 209 nm in the spectrum of YidC solubilized in C_{12}PC originates from the interaction of the detergent with periplasmic domain P1.

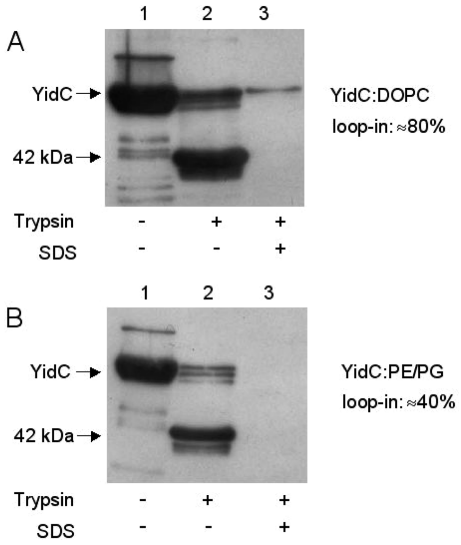

FIGURE 4: Topological analysis of the reconstituted YidC. Proteoliposomes with YidC reconstituted in (A) DOPC and (B) DOPE/DOPG (3:1, w/w) vesicles were digested with trypsin. The undigested (lanes 1) and digested (lanes 2) samples are shown. The full-length YidC and the 42 kDa fragment are denoted with an arrow. The percentage of YidC that has the P1 domain located in the lumen of the proteoliposomes (loop-in) was calculated.

Membrane Topology of Reconstituted YidC. The membrane topology of the reconstituted samples was examined by trypsin digestion of the proteoliposomes. If YidC is reconstituted with its P1 domain inside the lumen ("loop-in" conformation), trypsin digestion generates a 42 kDa protected fragment (*15*) containing the first and second transmembrane motif as well as loop P1 (see Figure 1). This large fragment can then be recognized by the antiserum. If the protein is reconstituted in the inverted orientation, no such fragment is expected after digestion.

Figure 4 shows the results of the tryptic digest of YidC reconstituted in DOPC and DOPE/DOPG vesicles. For both samples, the 42 kDa fragment was detected in significant amounts (A and B, lane 2). Compared to the nondigested protein (lane 1), more than 80% of YidC in DOPC and ~40% of YidC in DOPE/DOPG vesicles was found in the loop-in conformation. Since the topology of the reconstituted YidC is mostly in the correct orientation, we focused on these proteoliposomes for the substrate binding assay. As a control, the tryptic digest of the SDS-solubilized proteoliposomes did not exhibit the 42 kDa fragment (lane 3). Taken together, the results show that a large percentage of YidC is reconstituted in an orientation with the P1 domain located in the lumen of the proteoliposomes.

Pf3W0 Coat Protein-Induced Conformational Change in YidC. Fluorometric titration was used to probe for tertiary structural changes of YidC upon binding to its substrate Pf3 coat. Panel 1A in Figure 5 shows a representative series of intrinsic Trp fluorescence spectra recorded after titration of 0.32 μM YidC solubilized in C_{12}PC with increasing amounts Pf3W0 coat. These

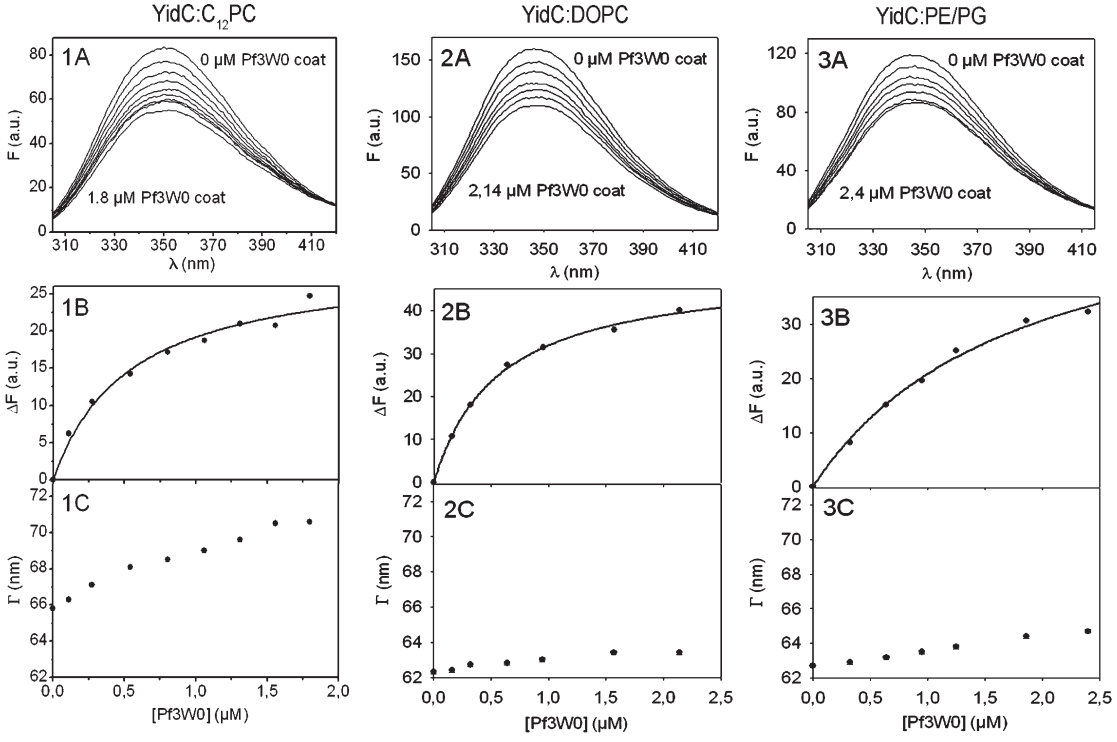

FIGURE 5: Series of intrinsic Trp fluorescence spectra recorded after the titration of (1A) 0.32 μM YidC in C_{12}PC micelles, (2A) 0.20 μM YidC reconstituted in DOPC vesicles, and (3A) 0.25 μM YidC reconstituted in DOPE/DOPG (3:1, w/w) vesicles with increasing amounts of Pf3W0 coat protein and the corresponding binding curves (1B−3B) constructed from the fluorescence values at 350 and 345 nm for the detergent-solubilized and reconstituted samples, respectively. The curves show a best-fit K_D value of (0.53 ± 0.10) μM for YidC in C_{12}PC [in 20 mM Tris-HCl (pH 8.0), 50 mM NaCl, 10% (v/v) 2-propanol, and 0.87 mM C_{12}PC] and K_D values of (0.66 ± 0.04) and (1.78 ± 0.27) μM for YidC in DOPC and DOPE/DOPG vesicles, respectively [in 20 mM Tris-HCl (pH 7.0), 10% (v/v) 2-propanol, and 100 mM NaCl for YidC in DOPC and 250 mM NaCl for YidC in DOPE/DOPG vesicles]. (1C−3C) Dependence of line width Γ (see eq 1) of the YidC fluorescence spectra in section A on Pf3W0 coat protein concentration.

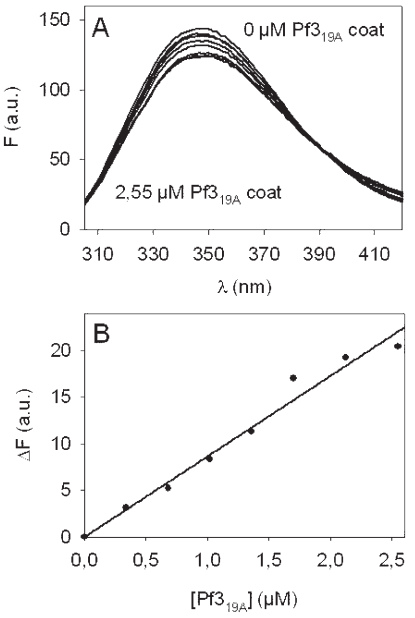

FIGURE 6: (A) Series of intrinsic Trp fluorescence spectra recorded after the titration of 0.20 μM YidC reconstituted in DOPC vesicles with increasing amounts of $Pf3_{19A}$ coat protein and (B) binding curve constructed from the fluorescence values at 345 nm [in 20 mM Tris-HCl (pH 7.0), 100 mM NaCl, and 10% (v/v) 2-propanol].

spectra reveal that the fluorescence of the Trp residues decreases upon binding of Pf3W0 coat to the YidC insertase. The binding curve (Figure 5, panel 1B) constructed from the fluorescence values at 350 nm could be fitted with good accuracy to eq 2 with a best-fit value for dissociation constant K_D of (0.53 ± 0.10) μM. Data analysis from two consecutive experiments revealed a mean K_D value of (0.67 ± 0.14) μM. The quenching of the Trp fluorescence is accompanied by a broadening of the fluorescence spectra from a Γ of 65.8 nm (0 μM Pf3W0 coat) to a Γ of 70.6 nm upon addition of Pf3W0 coat protein (1.8 μM Pf3W0 coat) as shown in panel 1C in Figure 5. The emission maximum λ_{max} was not significantly shifted (< 1 nm) in this experiment.

A similar quenching behavior was measured for the membrane-reconstituted YidC in DOPC. A series of intrinsic Trp fluorescence spectra were recorded after titration of 0.20 μM reconstituted YidC with Pf3W0 coat, and the binding curve was constructed from the fluorescence values at 345 nm (Figure 5, panels 2A and 2B). The binding curve could be fitted with good accuracy to eq 2 with a best-fit value for dissociation constant K_D of (0.66 ± 0.04) μM. Data analysis from two consecutive experiments revealed a mean K_D value of (0.61 ± 0.06) μM. In contrast to that of the C_{12}PC-solubilized protein, the line width changed only slightly from a Γ of 62.3 nm (0 μM Pf3W0 coat) upon the addition of the Pf3W0 coat protein to a Γ of 63.4 nm (2.14 μM Pf3W0 coat) (Figure 5, panel 2C).

For a control, YidC reconstituted in DOPC vesicles was titrated with $Pf3_{19A}$ coat protein. The hydrophobic membrane anchor of this mutant is replaced by a 19-residue polyalanine sequence and does not insert into the *E. coli* membrane in vivo (*22*). A series of intrinsic fluorescence spectra were recorded after titration of 0.20 μM YidC with increasing amounts of $Pf3_{19A}$ coat (Figure 6A). The spectra show that the intrinsic fluorescence decreases upon addition of the $Pf3_{19A}$ coat to the insertase. The accurate linear behavior of the binding curve (Figure 6B) constructed from the fluorescence values at 345 nm indicates a nonspecific binding of this Pf3 coat mutant to YidC.

When the substrate binding experiment was performed with YidC reconstituted in DOPE/DOPG vesicles under conditions identical to those used in the experiment with the DOPC vesicles [20 mM Tris-HCl (pH 7.0), 100 mM NaCl, and 10% (v/v) 2-propanol], data of poor quality were obtained (data not shown). However, at a salt concentration of > 200 mM NaCl, the quality of the binding curves became acceptable. This behavior is plausible considering the different charge distributions of the PE/PG headgroups as compared to DOPC (see Discussion). Panel 3A in Figure 5 shows a series of intrinsic Trp fluorescence spectra recorded after titration of 0.25 μM reconstituted YidC in the same buffer mentioned above in the presence of 250 mM NaCl. The binding curve constructed from the fluorescence values at 345 nm could be fitted with good accuracy to eq 2 with a best-fit value for dissociation constant K_D of (1.78 ± 0.25) μM (Figure 5, panel 3B). The observed broadening of the spectra after titration was nearly twice the value that was determined for YidC in DOPC membranes. The line width changed from a Γ of 62.7 nm (0 μM Pf3W0 coat) upon the addition of the Pf3W0 coat protein to a Γ of 64.7 nm (2.4 μM Pf3W0 coat) (Figure 5, panel 3C). However, this broadening is still 2−3 times less than that observed for the solubilized YidC. In both experiments, with DOPC and with DOPE/DOPG-reconstituted YidC, the emission maximum λ_{max} was not significantly shifted (< 1 nm).

The observed quenching of the Trp fluorescence is consistent with a conformational change in the YidC protein upon binding to its substrate. This quenching is concomitant with a spectral broadening of the Trp fluorescence band which is reduced as compared to that of the detergent-solubilized protein. Furthermore, the absence of a spectral shift in all experiments suggests that the accessibility of the Trp residues to the solvent remained unchanged upon Pf3 coat binding.

Pf3W0 Coat-Induced Conformational Change in $YidC_{W332/W334}$ and $YidC_{W454}$. To investigate which of the Trp residues are mainly involved by the quenching process, two YidC mutants were examined: (i) $YidC_{W332/W334}$ with only two Trp residues in the P1 domain at positions 332 and 334 and (ii) $YidC_{W454}$ with a single Trp residue at position 454 in the second periplasmic loop between transmembrane regions TM3 and TM4 (see Figure 1).

Panels 1A and 2A of Figure 7 show representative series of intrinsic Trp fluorescence spectra recorded after titration of 0.18 μM $YidC_{W332/W334}$ and 0.2 μM $YidC_{W454}$ reconstituted in DOPC vesicles, respectively, with increasing amounts of Pf3W0 coat. Because of the lower Trp content of both YidC mutants, the fluorescence spectra exhibit a considerably lower signal-to-noise ratio compared to the spectra of the wild type (see Figure 5). The binding curves (Figure 7, panels 1B and 2B) constructed from the fluorescence values at 345 nm could be fitted with sufficient accuracy to eq 2 with a best-fit values for dissociation constant K_D of (0.95 ± 0.28) and (0.30 ± 0.04) μM for $YidC_{W332/W334}$ and $YidC_{W454}$, respectively. The spectrum of unbound $YidC_{W332/W334}$ (0 μM Pf3W0 coat) shows an emission maximum λ_{max} of 344 nm which slightly changes upon titration (< 2 nm). In contrast, the fluorescence emission for $YidC_{W454}$ shows a maximum λ_{max} of 342 nm (0 μM Pf3W0 coat) which is red-shifted by ≈4 nm upon addition of substrate (2.1 μM Pf3W0 coat). Analysis of the fluorescence data revealed that the initial intensity of $YidC_{W332/W334}$ is quenched by 26 ± 3%, whereas the intensity for $YidC_{W454}$ is quenched by 36 ± 2% upon addition of the substrate. This result indicates that the surroundings of Trp residue W454 are

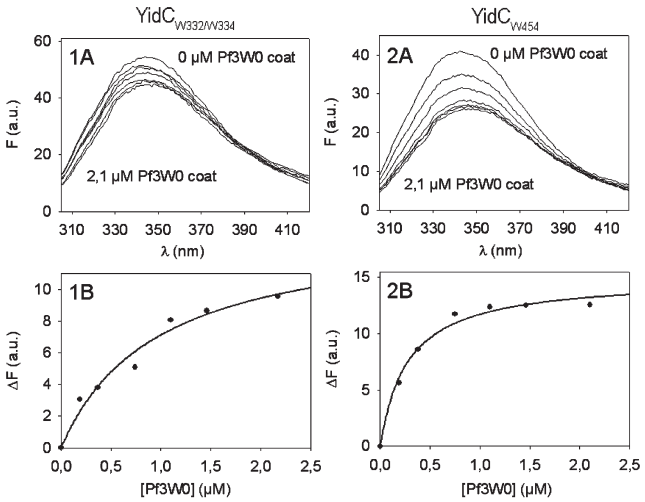

FIGURE 7: Series of intrinsic Trp fluorescence spectra recorded after the titration of (1A) 0.18 μM YidC$_{W332/W334}$ and (2A) 0.20 μM YidC$_{W454}$, both reconstituted in DOPC vesicles, with increasing amounts of Pf3W0 coat protein and corresponding binding curves (1B and 2B) constructed from the fluorescence values at 345 nm [in 20 mM Tris-HCl (pH 7.0), 100 mM NaCl, and 10% (v/v) 2-propanol].

subjected to a larger conformational change than the surroundings of Trp residues W332 and W334 in the large periplasmic region.

DISCUSSION

YidC and its substrate Pf3 coat make up a well-examined model system for the Sec-independent pathway of membrane insertion. The initial step of such an insertion process is the binding of the substrate to the insertase. This step is often considered to be an irrevesible binding process. However, in a previous study, we had shown unambiguously by fluorometric titration of ANS-labeled YidC that the Pf3 coat protein binds reversibly to detergent-solubilized YidC (*10*). To obtain binding data for the native system, we used in this study YidC that was reconstituted in DOPC and DOPE/DOPG membranes. Instead of labeling the insertase with ANS, which may pose problems because of the partitioning of the ANS molecules into the hydrophobic interior of the membrane, we have used the fluorescence properties of the YidC's Trp residues. Since the fluorescence properties of Trp are highly sensitive to even minor changes in the local environment, changes in the fluorescence yield and spectral position of the intrinsic fluorescence are direct indications of conformational events of a protein. We have taken advantage of the fact that the 11 Trp residues of YidC together with a sensitive photodetection system allow fluorometric titration experiments with reconstituted YidC at protein concentrations in the range of ~100 nM to be performed with a sufficient signal level.

The measured dependence of the intrinsic Trp fluorescence of YidC on the concentration of the added Pf3 coat protein (Figure 5, panels 1A−3A) allowed the description of the substrate binding process. All binding curves constructed from the fluorescence data showed a similar hyperbolic, noncooperative behavior and K_D values (≈1 μM) in the same range that was measured previously in experiments with ANS-labeled YidC (*10*). In conclusion, the binding behavior of the reconstituted samples confirms our results obtained with detergent-solubilized YidC. In the experiments with YidC reconstituted in DOPE/DOPG vesicles, we found that the Trp emission spectra exhibited poor reproducibility under conditions that were used in the experiments with DOPC proteoliposomes. We think that this behavior can be explained with the charge distribution of the Pf3 coat protein and the phospholipid headgroups. Pf3 coat protein has two positively charged amino acid residues at its C-terminus which are predicted to bind to the inner membrane surface prior to its insertion (*23*, *24*). The headgroups of the phospholipid membrane comprised of DOPE and DOPG (3:1, w/w) have charge distributions similar to that of the bacterial inner membrane, suggesting that Pf3 coat can electrostatically bind to the membrane surface. This binding event may lead to agglomeration of proteoliposomes resulting in a disturbed diffusion behavior of the sample as well as to sedimentation of the agglomerated proteoliposomes leaving the detection volume of the cuvette. This was tested by analyzing the binding at elevated NaCl concentrations which may result in an increased level of shielding of the membrane surface potential of the negatively charged PG headgroups with increasing salt concentrations (*25*, *26*). We noticed that at >200 mM NaCl the recorded spectra became reproducible, allowing the construction of binding curves of reliable quality. Thus, most probably, the electrostatic binding between the Pf3 coat protein and the phospholipid headgroups is the reason why we obtained data of good quality only at high salt concentrations which prevent such undesired electrostatic interactions. Because of the observed quenching of the Trp fluorescence together with the particular arrangement of the Trp residues (see Figure 1), we conclude that the substrate-binding site, which is located in the cytoplasmic part of the insertase, is conformationally coupled to the periplasmic region of the insertase. In the experiments with Trp mutants YidC$_{W332/W334}$ and YidC$_{W454}$ reconstituted in DOPC vesicles, we attempted to locate the periplasmic regions that are subjected to the conformational change. The results indicate that the structural change caused by the binding process involves mainly the membrane-spanning domain and also, to a less degree, periplasmic domain P1.

We found that the surrounding environment also affects the intrinsic Trp fluorescence of YidC. The fluorescence spectra of YidC in membranes as well as of YidC solubilized in DDM are clearly blue-shifted compared to that of YidC solubilized with C_{12}PC (Figure 2). A blue shift of the Trp fluorescence is typically a sign of decreased accessibility of the residues to the aqueous surroundings. However, the experimental data do not allow us to distinguish between a change in the tertiary structure or an increase in the level of shielding of the Trp residues by the lipid and DDM molecules, respectively. The analysis of the line shapes revealed that the line width of the intrinsic fluorescence is appreciably reduced upon membrane reconstitution, and the substrate binding process involves a line broadening (Figure 5, panels 1C−3C) which turned out to be smaller for the membrane-reconstituted samples. These results are consistent with the idea that the lateral pressure of the membrane reduces the dynamics and accessible conformational space of a membrane protein (*27*).

CD spectroscopy was used to analyze the conformational state of YidC before and after membrane reconstitution. The spectra in Figure 3 reveal the influence upon different environments on the YidC secondary structure. Compared to that of the solubilized state, the CD spectra for the reconstituted protein changed significantly. An exact calculation of the fractions of secondary structure elements in membrane proteins is difficult to obtain by analyzing CD spectra (*28*). However, the results clearly show that the fraction of α-helical structure of YidC is increased due to the interactions with the detergent molecules. The CD spectra of the

reconstituted YidC in DOPC and YidC in DOPE/DOPG vesicles are similar in shape and amplitude, so these two environments can be considered as equivalent. Since the DOPE/DOPG membranes (3:1, w/w) used for the reconstitution have a composition similar to that of the *E. coli* inner membrane, we believe that the spectra in Figure 3B represent the native conformation of the YidC protein.

Since the reconstituted YidC in DOPC and the detergent-solubilized YidC exhibited nearly identical K_D values for the Pf3 coat protein, one might conclude that $C_{12}PC$ is a good choice for solubilizing YidC in a functional state. However, the CD analysis shows an unambiguously strong influence of $C_{12}PC$ on the secondary structure of the YidC P1 domain (Figure 3A,C). The appearance of a negative band around 206 nm suggests that the interaction of $C_{12}PC$ with the P1 domain increases the α-helical content. Although periplasmic domain P1 is not required for the insertase function of YidC (*29*), we do not recommend the use of this detergent.

The knowledge of the K_D value for the initial binding process allows us to give an estimate for the rate that determines the velocity of the actual insertion event. The overall process can be described by the scheme

$$\mathrm{YidC} + \mathrm{Pf3}_{\mathrm{free}} \underset{k_{-1}}{\overset{k_1}{\rightleftharpoons}} \mathrm{YidC \cdot Pf3} \xrightarrow{k_2} \mathrm{YidC} + \mathrm{Pf3}_{\mathrm{transmembrane}}$$

where k_1, k_{-1}, and k_2 represent the velocity constants for the individual reactions. In this scheme, the association process described by k_1 is assumed to be diffusion-controlled and the insertion process described by k_2 is considered to be irreversible. The order of magnitude of association rate k_1 is estimated with the Smolukowski equation for bimolecular collision to be $\sim 10^8\ M^{-1}\ s^{-1}$, and with the equation $1\ \mu M \approx K_D = k_{-1}/k_1$, we obtain a value for the dissociation rate of the YidC·Pf3 complex (k_{-1}) of $\approx 10^2\ s^{-1}$. This high value of k_{-1} suggests that in vivo, the insertion rate k_2 should be at least 1 order of magnitude higher, i.e., $k_2 \approx 10^3\ s^{-1}$. This value is similar to the turnover rates of, for example, fumarase and β-lactamase (*30*). Future experiments will attempt to define exactly the membrane insertion rate of the Pf3 coat protein.

ACKNOWLEDGMENT

We thank Prof. Irmgard Sinning for providing plasmid pET24-P1D and Prof. Robin Ghosh for fruitful discussions and critical review of the manuscript. We also thank Lutz Tessmer for technical assistance with the protein purification.

REFERENCES

1. Kuhn, A., Stuart, R., Henry, R., and Dalbey, R. E. (2003) The Alb3/Oxa1/YidC protein family: Membrane-localized chaperones facilitating membrane protein insertion?. *Trends Cell Biol. 13*, 510–516.
2. Sääf, A., Monne, M., de Gier, J. W. L., and von Heijne, G. (1998) Membrane Topology of the 60-kDa Oxa1p Homologue from *Escherichia coli*. *J. Biol. Chem. 273*, 30415–30418.
3. Kuhn, A. (2009) From the Sec complex to the YidC insertase. *Biol. Chem.* accepted manuscript, DOI: 10.1515/BC.2009.059.
4. Kuhn, A. (1995) Bacteriophage Pf3 and M13 as model systems for Sec-independent protein transport. *FEMS Microbiol. Rev. 17*, 185–190.
5. van der Laan, M., Bechtluft, P., Kol, S., Nouwen, N., and Driessen, A. J. (2004) F_1F_o ATP synthase subunit c is a substrate of the novel YidC pathway for membrane protein biogenesis. *J. Cell Biol. 165*, 213–222.
6. Facey, S. J., Neugebauer, S. A., Krauss, S., and Kuhn, A. (2007) The mechanosensitive channel protein MscL is targeted by the SRP to the novel YidC membrane insertion pathway of *Escherichia coli*. *J. Mol. Biol. 365*, 995–1004.
7. Price, C. E., and Driessen, A. J. (2008) YidC is involved in the biogenesis of anaerobic respiratory complexes in the inner membrane of *Escherichia coli*. *J. Biol. Chem. 283*, 26921–26927.
8. Kiefer, D., and Kuhn, A. (1999) Hydrophobic forces drive spontaneous membrane insertion of the bacteriophage Pf3 coat protein without topological control. *EMBO J. 18*, 6299–6306.
9. Klenner, C., Yuan, J., Dalbey, R. E., and Kuhn, A. (2008) The Pf3 coat protein contacts TM1 and TM3 of YidC during membrane biogenesis. *FEBS Lett.*, 3967–3972.
10. Gerken, U., Erhardt, D., Bär, G., Ghosh, R., and Kuhn, A. (2008) Initial binding process of the membrane insertase YidC with its substrate Pf3 coat protein is reversible. *Biochemistry 47*, 6052–6058.
11. Lessl, M., Balzer, D., Lurz, R., Waters, V. L., Guiney, D. G., and Lanka, E. (1992) Dissection of IncP conjugative plasmid transfer: Definition of the transfer region Tra2 by mobilization of the Tra1 region in trans. *J. Bacteriol. 174*, 2493–2500.
12. Martinez Molina, D., Lundbäck, A. K., Niegowski, D., and Eshaghi, S. (2008) Expression and purification of the recombinant membrane protein YidC: A case study for increased stability and solubility. *Protein Expression Purif. 62*, 49–52.
13. Ravaud, S., Stjepanovic, G., Wild, K., and Sinning, I. (2008) The crystal structure of the periplasmic domain of the *Escherichia coli* membrane protein insertase YidC contains a substrate binding cleft. *J. Biol. Chem. 283*, 9350–9358.
14. Lowry, O. H., Rosebrough, N. J., Farr, A. L., and Randall, R. J. (1951) Protein measurement with the Folin phenol reagent. *J. Biol. Chem. 193*, 265–275.
15. Serek, J., Bauer-Manz, G., Struhalla, G., van den Berg, L., Kiefer, D., Dalbey, R. E., and Kuhn, A. (2004) *Escherichia coli* YidC is a membrane insertase for Sec-independent proteins. *EMBO J. 23*, 295–301.
16. Gerken, U., Lupo, D., Tietz, C., Wrachtrup, J., and Ghosh, R. (2003) Circular symmetry of the light-harvesting 1 complex from *Rhodospirillum rubrum* is not perturbed by interaction with the reaction center. *Biochemistry 42*, 10354–10360.
17. Ames, B. N., and Dubin, D. T. (1960) The role of polyamines in the neutralization of bacteriophage deoxyribonucleic acid. *J. Biol. Chem. 235*, 769–775.
18. Rigaud, J. L., Paternostre, B., and Bluzat, A. (1988) Mechanisms of membrane protein insertion into liposomes during reconstitution procedures involving the use of detergents. 2. Incorporation of the light-driven proton pump bacteriorhodopsin. *Biochemistry 27*, 2677–2688.
19. Wallace, B. A., and Mao, D. (1984) Circular dichroism analyses of membrane proteins: An examination of differential light scattering and absorption flattening effects in large membrane vesicles and membrane sheets. *Anal. Biochem. 42*, 317–328.
20. Ladokhin, A. S., Jayasinghe, S., and White, A. (2000) How to measure and analyze tryptophan fluorescence in membranes properly, and why bother?. *Anal. Biochem. 285*, 235–245.
21. Oliver, D. C., and Paetzel, M. (2007) Crystal structure of the major periplasmic domain of the bacterial membrane protein assembly facilitator YidC. *J. Biol. Chem. 283*, 5208–5216.
22. Xie, K., Hessa, T., Seppalä, S., Rapp, M., von Heijne, G., and Dalbey, R. E. (2007) Features of transmembrane segments that promote the lateral release from the translocase into the lipid phase. *Biochemistry 46*, 15153–15161.
23. Gallusser, A., and Kuhn, A. (1990) Initial steps in protein membrane insertion. Bacteriophage M13 procoat protein binds to the membrane surface by electrostatic interaction. *EMBO J. 9*, 2723–2729.
24. Kiefer, D., Hu, X., Dalbey, R., and Kuhn, A. (1997) Negatively charged amino acid residues play an active role in orienting the Sec-independent Pf3 coat protein in the *Escherichia coli* inner membrane. *EMBO J. 16*, 2197–21204.
25. Eisenberg, M., Gresalfi, T., Riccio, T., and McLaughlin, S. (1979) Adsorption of monovalent cations to bilayer membranes containing negative phospholipids. *Biochemistry 18*, 5213–5223.
26. Loosley-Millman, M. E., Rand, R. P., and Parsegian, V. A. (1981) Effects of monovalent ion binding and screening on measured electrostatic forces between charged phospholipid bilayers. *Biophys. J. 40*, 221–232.
27. Gerken, U., Jelezko, F., Götze, B., Tietz, C., Branschädel, M., Ghosh, R., and Wrachtrup, J. (2003) Membrane environment reduces the accessible conformational space available to an integral membrane protein. *J. Phys. Chem. B 107*, 338–343.
28. Wallace, B. A., Lees, J. G., Orry, A. J. W., Lobley, A., and Janes, R. W. (2003) Analyses of circular dichroism spectra of membrane proteins. *Protein Sci. 12*, 875–884.
29. Xie, K., Kiefer, D., Nagler, G., Dalbey, R. E., and Kuhn, A. (2006) Different regions of the nonconserved large periplasmic domain of *Escherichia coli* YidC are involved in the SecF interaction and membrane insertase activity. *Biochemistry 45*, 13401–13408.
30. Fersht, A. (1985) Enzyme Structure and Mechanism, W. H. Freeman and Co., New York.